INTERNATIONAL SOCIETY FOR SOIL MECHANICS AND GEOTECHNICAL ENGINEERING



This paper was downloaded from the Online Library of the International Society for Soil Mechanics and Geotechnical Engineering (ISSMGE). The library is available here:

https://www.issmge.org/publications/online-library

This is an open-access database that archives thousands of papers published under the Auspices of the ISSMGE and maintained by the Innovation and Development Committee of ISSMGE.

The paper was published in the proceedings of the 20th International Conference on Soil Mechanics and Geotechnical Engineering and was edited by Mizanur Rahman and Mark Jaksa. The conference was held from May 1st to May 5th 2022 in Sydney, Australia.

Energy-based evaluation of liquefaction-induced strain and settlement

Évaluation basée sur l'énergie de la déformation et du tassement induits par la liquéfaction

Takaji Kokusho

Chuo University, Bunkyo-ku, Tokyo, Japan

ABSTRACT: Energy-Based Method (EBM) for liquefaction potential evaluation was previously developed, wherein the total demand to be compared with the capacity at a site can be given by earthquake upward SH-wave energy. To make the most of the EBM where the energy demand is given, evaluation steps are added here as a second stage to calculate the liquefaction-induced strain and associated soil settlement by introducing a simple assumption that the wave energy is equally shared among layers which attain initial liquefaction. By applying this to a case history site, the second stage liquefaction evaluation tends to calculate much higher shear strains than 7.5% corresponding to the initial liquefaction in a smaller number of layers than in the first stage. Furthermore, soil subsidence calculated using a volumetric strain versus shear strain correlations for intact soils is found agreeable with actual performance in the case history. Thus, two-stage EBM of liquefaction evaluation can practically predict not only liquefaction potential but also induced strain and surface settlement without resorting to nonlinear numerical analyses.

RÉSUMÉ: Une méthode basée sur l'énergie (EBM) pour l'évaluation du potentiel de liquéfaction a été précédemment développée, dans laquelle la demande totale par rapport à la capacité d'un site peut être donnée par l'énergie des ondes SH d'un tremblement de terre. Pour tirer le meilleur parti de l'EBM où la demande d'énergie est donnée, des étapes d'évaluation sont ajoutées ici en tant que deuxième étape pour calculer la déformation induite par la liquéfaction et le tassement du sol associé en introduisant une hypothèse simple que l'énergie des vagues est également partagée entre les couches qui atteignent liquéfaction initiale. En appliquant ceci à un site d'histoire de cas, l'évaluation de liquéfaction de deuxième étape tend à calculer des déformations de cisaillement beaucoup plus élevées que 7,5% correspondant à la liquéfaction initiale dans un plus petit nombre de couches que dans la première étape. De plus, la sous-évidence du sol calculée en utilisant une corrélation entre la déformation volumétrique et la déformation de cisaillement pour les sols intacts est jugée conforme à la performance réelle dans l'histoire de cas. Ainsi, l'EBM en deux étapes de l'évaluation de la liquéfaction peut pratiquement prédire non seulement le potentiel de liquéfaction, mais aussi la déformation induite et le tassement de surface.

KEYWORDS: Energy-based evaluation; wave energy; dissipated energy; induced strain; liquefaction-induced settlement.

1 INTRODUCTION

The common basis of energy-based liquefaction evaluation methods (EBM) so far proposed is to compare energy capacity for liquefaction with energy demand of design earthquakes, similar to the currently employed stress-based method (SBM). The energy capacity is determined from dissipated energy for soils to reach the state of liquefaction during seismic loading. Among them, Davis & Berrill (1982) and Kazama et al. (1999) proposed EBM, wherein the earthquake demand energy was not directly calculated, but calculated from empirical formula and one-dimensional response analyses, respectively.

Kokusho (2013) and Kokusho & Mimori (2015) developed another type of EBM wherein, unlike others, upward seismic wave energies reaching individual layers are quantified and compared with the dissipated energies. Its theoretical background was discussed in Kokusho (2017) on how to evaluate energies of design motions and compare with dissipated energies using laboratory soil test data. The results demonstrated that, for several ground motions, EBM tends to be roughly compatible with the stress-based method (SBM), if stress reduction coefficients r_n (similar to Magnitude Scaling Factor in USA) are appropriately chosen in SBM. However, the gap between them tended to widen for ground motions with exceptionally large or small energy compared to corresponding acceleration wherein EBM successfully reproduced actual field performance, whereas SBM could not properly appreciate the great impact of energy.

One of remarkable features of the present EBM is that the total energy demand for liquefaction can be quantified at a site if a design earthquake is given (Kokusho 2017). That may allow one not only to know if soil layers of a site will liquefy or not but also how large liquefaction-induced strain develops in a simplified evaluation without resorting to complicated effective stress non-linear dynamic response analyses.

In this paper, following the evaluation steps of the EBM previously proposed, steps will be added to evaluate not only the potential of liquefaction but also how large strain is induced in those liquefied layers by introducing a simple rule on how the total wave energy is allocated among multiple liquefiable layers. Furthermore, liquefaction-induced soil settlement is calculated from the induced strain using an empirical correlation between volumetric strain and maximum shear strain. Then, a soil model of liquefaction case-history site employed in the previous research are revisited to evaluate induced strains and associated settlement to compare with the actual performance.

2 LIQUEFACTION EVALUATION STEPS OF EBM

The evaluation steps of EBM previously proposed (Kokusho 2013) using upward wave energy as energy demand are outlined as follows. Some of the experimental equations already published is updated in this paper by utilizing more recent research findings on in situ intact samples as mentioned below.

STEP-1:

At a given site, a soil profile consisting of different soil types is divided into layers of identical thickness H=1 or 2 m throughout the soil model in accordance with penetration test data. CRR-values employed in SBM are determined in individual layers based on the corresponding penetration resistance.

STEP-2:

Normalized cumulative dissipated energy (abbreviated as dissipated energy hereafter) $\sum \Delta W/\sigma_c'$ for a soil of a unit volume to attain initial liquefaction (corresponding to maximum double amplitude axial strain $\varepsilon_{DA\,{
m max}}=5\%$ in triaxial tests or maximum

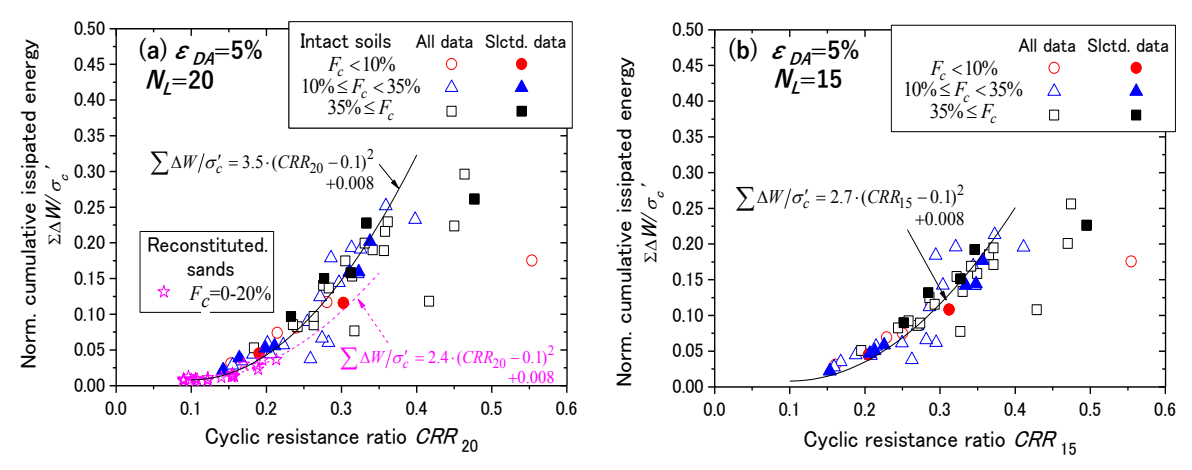


Figure 1: Dissipated energy versus cyclic resistance ratio by triaxial tests on intact samples: (a) CRR₂₀, (b) CRR₁₅

double amplitude shear strain $\gamma_{DA \max} = 7.5\%$ in simple shear tests) is determined in each layer from the *CRR*-value by using either of the following equations;

$$\sum \Delta W / \sigma_c' = 3.5 (CRR_{20} - 0.1)^2 + 0.008 \tag{1}$$

$$\sum \Delta W / \sigma_c' = 2.7 (CRR_{15} - 0.1)^2 + 0.008$$
 (2)

Here, the dimension of $\Sigma\Delta W$ is the energy per unit volume, and non-dimensionalized by effective confining stress σ'_c . CRR_{20} and CRR_{15} are the cyclic resistance ratios in SBM for the equivalent number of cycles for initial liquefaction, N_L =20 and 15, respectively. $\Sigma\Delta W/\sigma'_c$ should ideally be the same in Eqs. (1) and (2), if the uniqueness of dissipated energy for liquefaction holds irrespective of stress histories.

The equations have been developed by Tanimoto & Kokusho (2020) from a series of triaxial liquefaction tests on intact soils sampled from various sites in Japan (reported by Sasaki et al. 2016). They are a revised version of a following equation by Kokusho (2013) originally derived from a set of triaxial liquefaction tests on reconstituted loose sands.

$$\sum \Delta W / \sigma_c' = 2.4 (CRR_{20} - 0.1)^2 + 0.008 \tag{3}$$

In the reconstituted sands, the dissipated energy was almost uniquely correlated with induced strain irrespective of the cyclic stress ratio CSR or the number of cycles for liquefaction N_L (Kokusho 2013). However, intact samples from in situ were found to be quite different in their cyclic triaxial test results where the energy was not uniquely determined but decreasing with increasing CSR or decreasing N_L for larger induced strains in particular (Tanimoto & Kokusho 2020). This energy performance seems to be inherent to cyclic triaxial tests where the axial strain tends to grow larger asymmetrically in the extension side. It is quite different from in situ seismic stress condition which can be closely reproduced by a cyclic simple shear device, wherein stain tends to develop symmetrically. To overcome this problem, the dissipated energies for various CSR obtained by triaxial tests have been converted by an empirical formula to the energy corresponding to CRR=CSR at $N_L=20$ or 15, that is normally employed in SBM, and correlated with that particular CRR-value, the details of which are available in Tanimoto & Kokusho (2020).

Consequently, close correlations have been obtained as plotted in Figure 1(a) and Figure 1(b) for $CRR_{NL=20}$ and $CRR_{NL=15}$, respectively. The plots are all for intact sample data, among which

the close plots are for selected data with higher reliability. Eqs. (1) and (2) are regressed from the selected plots (both with the determination coefficient R^2 =0.92) as indicated with the solid curves in Figure 1. The star plots in the same diagram represent the results of reconstituted sand (Kokusho 2013) approximated by the dashed curve of Eq. (3).

Thus, the unique correlation Eq. (1) or (2) has been prepared between the energy $\Sigma \Delta W/\sigma'_c$ and CRR applicable to widely varying in situ soils of various soil types with different fines content and plasticity.

STEP-3:

Normalized cumulative strain energy $\sum W_{-}^{*}/\sigma_{c}^{\prime}$ (abbreviated as strain energy hereafter) compensating the above-mentioned dissipated energy $\sum \Delta W/\sigma_{c}^{\prime}$ is approximated as;

$$\sum W_{-}^{*} / \sigma_{c}' = 2 \times \sum \Delta W / \sigma_{c}' \tag{4}$$

The theoretical background of this equation was discussed in detail in Kokusho (2017), wherein the multiplier 2 in Eq. (4) has been proposed here as a round number of the triaxial test results including undisturbed samples (JGS committee report 2019).

STEP-4:

Liquefaction energy capacity (energy per area in dimension) in a layer of thickness H is calculated as $\sum W_-^*H$ from Eq. (4) using $\sum \Delta W/\sigma_c'$ corresponding to initial liquefaction, where the effective confining stress σ_c' is $\sigma_c' = (1+2K_0)\sigma_v'/3$, K_0 =earth-pressure coefficient at rest, and σ_v' =effective overburden.

STEP-5:

The upward wave energy E_u (energy per area in dimension) is calculated from an equivalent linear one-dimensional SH-wave propagation analysis in a soil profile at a given site using \dot{u} =particle velocity of upward wave, ρV_s =impedance of SH wave, and ultimate energy at the end of shaking E_{uf} is determined in each layer as (Kokusho 2017);

$$E_{uf} = \rho V_s \int_0^t (\dot{u})^2 dt \tag{5}$$

where the integration is implemented for the time duration of major motion $0 \sim t$ of a design earthquake.

STEP-6:

Energy ratio ΣW .* H/E_{uf} is calculated in each layer using the values ΣW .*H and E_{uf} above. A layer with smaller energy ratio has higher and earlier liquefaction potential than others in a given soil profile. The energy ratios of individual layers are numbered sequentially starting from the lowest ratio (i=1) toward the higher ones and summed up in terms of i as $\Sigma_i(\Sigma W$.* $H/E_{uf})_i$, which is denoted here as AER (accumulated energy ratio). Liquefaction occurs in that sequence and exclusively in those layers where;

$$AER = \sum_{i} (\sum W_{-}^{*} H / E_{uf})_{i} \le 1.0$$
 (6)

It is because the upward energy is considered to liquefy individual layers in the above-mentioned sequence until it is totally consumed by the liquefaction in that soil profile.

3 ENERGY-BASED INDUCED STRAIN EVALUATION

In the evaluation STEP-1~6 above, named here as the first evaluation stage, the energy capacity was defined corresponding to $\varepsilon_{DA\,{\rm max}}$ =5% or $\gamma_{DA\,{\rm max}}$ =7.5% (initial liquefaction) in each layer, and the maximum extent of liquefaction-prone layers was determined so that the energy demand can meet the capacity.

A remarkable feature of the present EBM is that the total energy demand for liquefaction can be prescribed at a site if a design earth quake is given, allowing one not only to evaluate whether individual soil layers of a site will liquefy or not but also how large liquefaction-induced strains develop there. It will become possible to calculate the strains even when multiple layers are liquefiable if a rule is adopted on how the upward energy is allocated among those layers. However, that kind of universal rule is by no means easy to establish because the energy distribution seems to be very much dependent on soil profiles, input seismic motions and nonlinear soil properties. Nonlinear dynamic response effective stress analyses based on rigorous constitutive laws may possibly provide the solution, that is not relevant in a simplified liquefaction evaluation.

Here, instead of postulating the same induced strain of γ_{DA} =7.5% corresponding to initial liquefaction as in the first stage evaluation, a simple rule is introduced here that the wave energy is equally shared among those layers which were judged as liquefiable as AER<1.0 in Eq. (6) in the first evaluation stage. It may well be expected that this rule despite its simplicity will lead the evaluation nearer to actual liquefaction behavior than in the first evaluation. Thus, steps in the second evaluation stage are described as follows.

STEP-7:

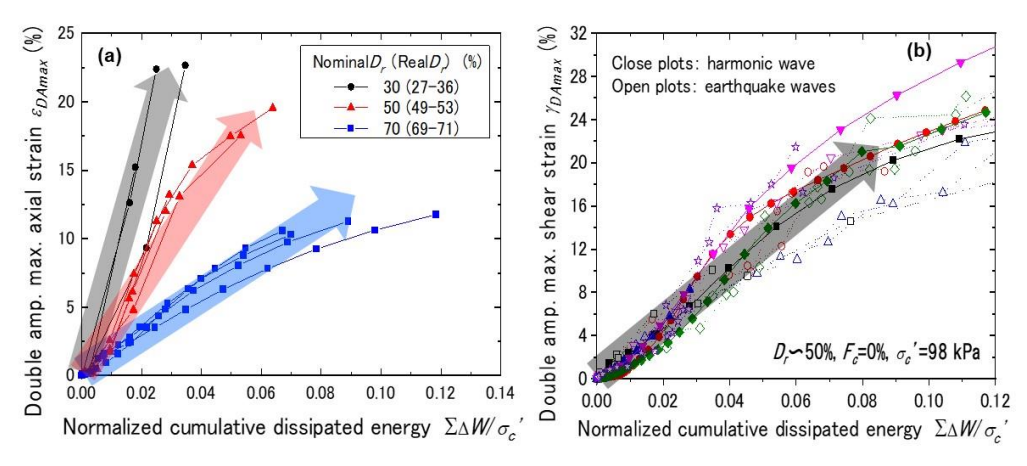


Figure 2. Dissipated energy versus DA strain during cyclic loading: (a) Triaxial tests on clean sand with three Dr-values, (b) Torsional shear tests on clean sand by harmonic and earthquake waves.

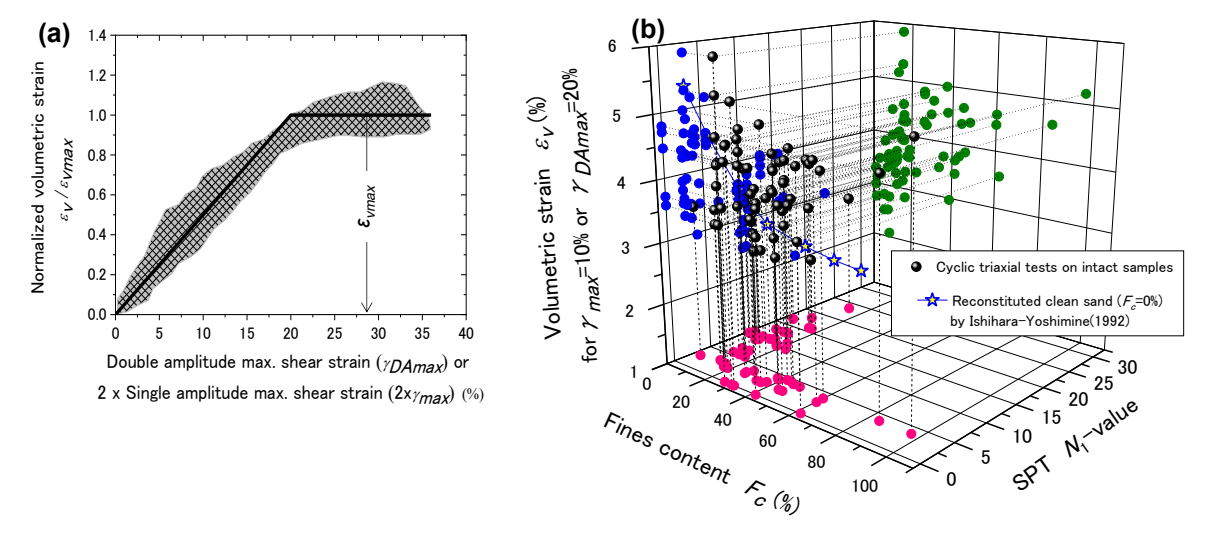


Figure 3. Conceptual correlation between volumetric strain and DA max. shear strain (a), and volumetric strain versus SPT N_1 value and fines content F_c by triaxial liquefaction tests on numerous intact samples (b).

The upward energy at a base layer is equally divided by m (the number of liquefied layers in the first stage), and the energy $\left(E_{uf}\right)_i/m$ comes up independently to each layer i to be consumed exclusively there.

STEP-8:

Maximum induced double amplitude shear strain in a liquefied layer i is calculated as follows;

$$\left(\gamma_{DA\,\text{max}}\right)_{i} = 7.5\% \times \left(\left(E_{uf}\right)_{i}/m\right) / \left(\sum W_{-}^{*}H\right)_{i} \tag{7}$$

Here, $\sum W_{-}^{*}H$ is the energy capacity for initial liquefaction corresponding to $\gamma_{DA \, \text{max}} = 7.5\%$. This equation stems from experimental results exemplified in Figure 2(a) for cyclic triaxial tests by harmonic motion on clean sand of different relative densities $D_r \approx 30$, 50 and 70% (Kokusho 2013). The double amplitude axial strain ε_{DAmax} is well correlated with dissipated energy $\Sigma \Delta W/\sigma_c$ ' in each D_r despite some data dispersions (presumably due to uncontrollable density fluctuations in the experiment), and may be approximated to be proportional as shown by the shaded arrows. Figure 2(b) depicts similar test data of γ_{DAmax} versus $\Sigma \Delta W/\sigma_c$ ' by torsional simple shear tests on clean sand of $D_r \approx 50\%$ wherein irregular loading of open symbols for 6 earthquake records compares with harmonic loading of close symbols (Kokusho & Kaneko 2018). Despite large data scatters in irregular loading in particular, the two groups of plots exhibit essentially consistent trends, and the uniqueness of energy in terms of induced strain regardless of different loading histories can be appreciable as a great merit of the energy-based evaluation. They can again be approximated by proportional relationship of the shaded arrow not only for harmonic waves but also for irregular earthquake waves. Hence, the proportional formula for induced strain in Eq. (7) seems possible, because $\Sigma \Delta W / \sigma_c$ and $\Sigma \Delta W / \sigma_c$ $\Sigma W_{-}^{*}/\sigma_{c}$ are also formulated to be proportional as already indicated in Eq. (4).

4 ENERGY-BASED SETTLEMENT EVALUATION

It is generally accepted that liquefaction-induced volumetric strain ε_{v} is closely correlated with associated maximum shear strain γ_{DAmax} . Ishihara & Yoshimine (1992) proposed a simple $\varepsilon_{v} \sim \gamma_{max}$ correlation (γ_{max} =maximum single amplitude shear strain) based on irregular loading simple shear tests on clean sand, wherein ε_{v} is idealized to be essentially proportional to γ_{max} up to a certain limit around γ_{max} =8~10%, and stays constant thereafter. This bilinear idealization of the $\varepsilon_{v} \sim \gamma_{max}$ relationship schematically shown in Figure 3(a) is employed here to calculate ε_{v} from γ_{DAmax} , where the upper limit of proportionality in shear strain is assumed as γ_{DAmax} =20% (γ_{max} =10%) and the volumetric strain in the vertical axis ε_{v} is normalized by that upper limit of volumetric strain ε_{vmax} as ε_{v} / ε_{vmax} .

There have been quite a few laboratory tests on the volumetric strain due to undrained cyclic loading, though most of them were conducted on reconstituted clean sands. In order to explore the $\varepsilon_V \sim \gamma_{DAmax}$ correlation more robust and applicable to in situ soils of various physical properties, the database by Sasaki et al. (2016) is utilized here. That consists of a great number of cyclic triaxial liquefaction tests of intact soils sampled from various natural and manmade ground in liquefied areas during the 2011 Tohoku earthquake, Japan, where almost all liquefaction-related parameters and post-liquefaction volume changes measured by burettes are available together with pertinent in situ test data mainly by Standard Penetration Tests. Among the SPT-related parameters, N_1 (corrected blow counts for effective overburden 98 kPa), F_c

(fines content) and G_c (gravel content) are selected here to conduct a multiple regression analysis utilizing the database for the volumetric strain $(\varepsilon_v)\gamma_{DAmax=20\%}$ corresponding to the maximum strain $\gamma_{DAmax}=20\%$. The regression study utilizing 66 test data of higher reliability in the database has yielded the formula (the determination coefficient $R^2=0.458$);

$$\left(\varepsilon_{\nu}\right)_{\gamma_{DA\text{max}}=20\%} = 3.85 - 0.0562 \times N_1 + 0.0120 \times F_c + 0.0290 \times G_c$$
 (8)

This indicates that the volumetric strain $(\varepsilon_v)_{\gamma_{DA\text{max}}=20\%}$ tends to increase with decreasing N_1 and increasing F_c , whereas G_c seems to have smaller impact because of smaller absolute value of G_c in non-gravelly soils.

In Figure 3(b), the value $(\varepsilon_{\nu})\gamma_{DAmax}=20\%$ are plotted in the vertical axis versus N_1 and F_c in the three-dimensional diagram. The plots are projected on the two-dimensional plane of $(\varepsilon_{\nu})\gamma_{DAmax}=20\%$ versus N_1 , and compared with the star plots for clean sand of $F_c=0$ which are read off for $\gamma_{max}=10\%$ ($\gamma_{DAmax}=20\%$) from a design chart proposed by Ishihara & Yoshimine (1992). The two kinds of plots essentially share a similar trend of volumetric strain decreasing with increasing N_1 -value, despite that widely varying fines content in the natural sands ($F_c=1\sim97\%$) seems to cause the data greatly dispersed. Thus, the evaluation steps for liquefaction-induced surface settlement can be possible as follows;

STEP-9:

Using the induced shear strains in individual layers determined in the previous step, the corresponding volumetric strains ε_v are calculated in proportion to γ_{DAmax} if $\gamma_{DAmax} \le 20\%$ as;

$$\varepsilon_{v} = \left(\varepsilon_{v}\right)_{\gamma_{DA\text{max}} = 20\%} \times \gamma_{DA\text{max}} / 20\% \tag{9}$$

If $\gamma_{DAmax} > 20\%$, it takes the upper limit determined in Eq. (8).

$$\varepsilon_{\nu} = \left(\varepsilon_{\nu}\right)_{\gamma_{D,4\text{max}} = 20\%} \tag{10}$$

STEP-10:

The ground surface settlement S can be obtained as the sum of layer i, involved in liquefaction as;

$$S = \sum_{i} S_{i} = \sum_{i} (\varepsilon_{v})_{i} H_{i} \tag{11}$$

Here, not only those beyond initial liquefaction ($\gamma_{DAmax} > 7.5\%$) but also those before are involved in calculating the settlement as long as they are judged liquefiable in the first evaluation stage.

5 CASE STUDY

During the 2011 Tohoku earthquake (*M*=9.0), reclaimed areas along the Tokyo bay, Japan, far from the epicenter, underwent widespread liquefaction. Takasu elementary school in Urayasu City, Chiba prefecture, was one of the typical sites focused in the previous paper (Kokusho & Mimori 2015), where extensive liquefaction occurred and induced large subsidence as photographed in Figure 4 (a). The soil consisted of landfill (B1, B2), hydraulic fill layer (F), alluvial sand (As1, As2) and clay (Ac, Nac) underlain by stiff gravelly base Dg at GL-43.7 m as indicated in Figure 4 (b). Fines contained in the soils in large percentage were assumed to be non-plastic, because ejecta coming out from liquefied sand containing lots of fines were all non-plastic.

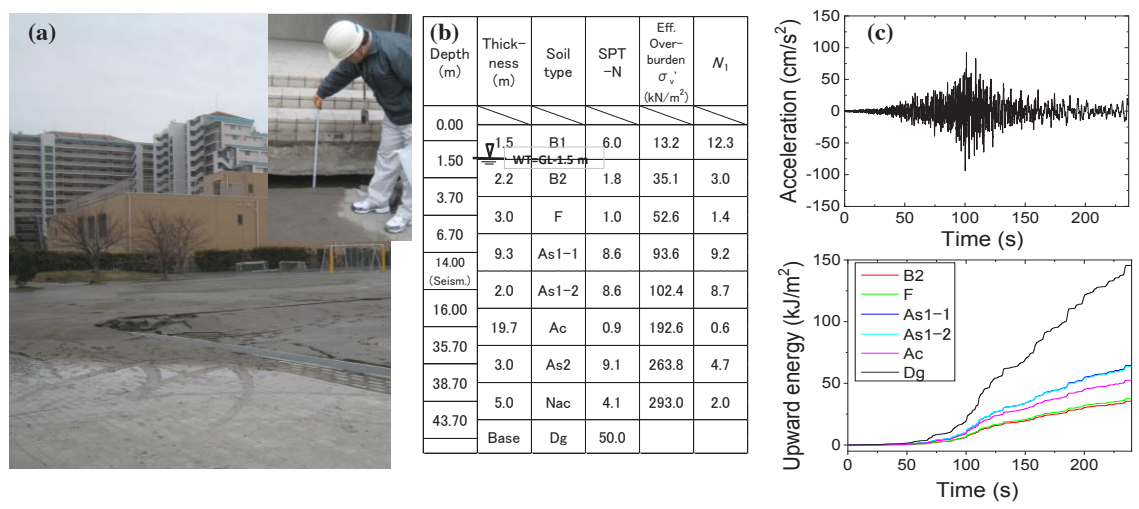


Figure 4. Photos of liquefaction of Takasu elementary school and soil settlement (a), Soil profiles (b), and input acceleration and upward energies (c).

Table 1. Liquefaction evaluation by EBM (compared with SBM), induced strain and settlement at Takasu elementary school liquefied site.

			Eff. overburden $\sigma_{v'}$ (kPa)	SPT-N1	nt	SBM (r _n =0.80)			EBM (H =1 m): Summation Σ for ΔW , W -* is abbreviated in EBM.										
	n (m)	Layer				CRR_{20} $ au_d/\sigma_c$ '	CSR $ au_{max}/\sigma_{v}$ '	F_s	1st stage evaluation						2nd stage evaluation				
Depth (m)					conter (%)				Liquefaction potential						Strain		Settlement		
Dent					Fines content F_c (%)				$\Delta W/\sigma_c'$	W^*/σ_c'	W*H (kJ/m³)	E_{uf} (kJ/m ²)	$W'H/E_{uf}$	AER	Liquefaction sequence	E_{uf}/m $m=11 \text{ (kJ/m}^2)$	У ДАтах (%)	$ \mathcal{E}_{V} (\%) for \mathcal{F}_{DAmax} = 20\% $	<i>E</i> ν× <i>H</i> (cm)
GL: 0 m																			
7	1.00	B1				0.257 0.25						36.81							
	2.00	B2	30.4	3.0			0.259	0.99	0.0939	0.188	3.81		0.103	0.513	8	3.35	6.6	4.31	1.42
WT=GL-1.5			38.2	3.0	52		_	0.44	0.0087	0.017	0.44		0.012	0.012		3.35	56.6	4.31	4.31
	4.00	F	45.5	1.4	95	0.184 0.31		0.51	0.0211	0.042	1.28	29.98	0.043	0.089	3	2.73	16.0	4.91	3.93
	5.00		51.4	1.4	95		0.314	0.59	0.0327	0.065	2.24		0.075	0.216	5	2.73	9.1	4.91	2.24
	6.00		57.3	1.4	95		_	0.51	0.0206	0.041	1.57		0.053	0.141	4	2.73	13.0	4.91	3.19
	7.00		64.0	9.2				0.86	0.1259	0.252	10.75	64.71	0.166	1.228	13	×	×	×	×
	8.00		72.9		23	0.361		1.10	0.2463	0.493	23.93		0.370	1.866	15	X	×	X	×
	9.00		81.7	9.2	23			0.77	0.0920	0.184	10.02		0.155	0.898	11	5.88	4.4	×	0.80
	10.00	As1-1	90.5	9.2			0.329 97	0.68	0.0620	0.124	7.49		0.116	0.743	10	5.88	5.9	X	1.06
	11.00 12.00		99.3	9.2 9.2	23			0.87	0.1311	0.262	17.37 5.87		0.268	1.497 0.307	14	5.88	7.5	×	1 0e
	13.00		108.2	9.2	23 52			0.60	0.0407	0.081	7.43		0.091	0.307	9	5.88	7.5 5.9	×	1.36 1.17
Seismo			125.8	9.2	52	_		0.63	0.0476	0.095	10.61		0.115	1.062	12	3.88 X	5.9 X	×	1.17 X
meter	15.00		134.6	8.7				0.69	0.0033	0.127	6.52		0.104	0.409	7	5.78	6.6	×	1.32
meter	16.00	As1-2	-2 143.5	8.7	52		- 0.390	0.49	0.0303	0.073	2.16	63.57	0.103	0.409	2	5.78	20.0	×	3.99
	10.00				J2	0.101		0.00	0.0113	0.020	2.10		0.004	0.040			Settlement		24.8

The equivalent linear one-dimensional SH-wave propagation analysis was carried out using a downhole acceleration record at 14 m below the ground surface in the EW-direction obtained by Earthquake Research Institute, University of Tokyo (Kokusho & Mimori 2015). As depicted in Figure 4 (c), recorded downhole maxumum acceleration was 0.096 g, and the upward wave energy calculated based on the SH-wave propagation analysis was E_{uf} =146 kJ/m² in the base layer at the end of the major motion.

Table 1 shows the soil model already developed in the previous research (Kokusho & Mimori 2015) for evaluating liquefaction potential in the top 16 m from the ground surface, comprising 16 layers of H=1 m each (with the top layer assumed unsaturated), together with pertinent parameters such as N_1 -values, F_c . The SBM results, unchanged from the previous research, are based on the road bridge design code in Japan (Japan Road Association 2017). Those layers with AER smaller than 1.0 in EBM and F_s smaller than 1.0 in SBM are judged as liquefiable and

shaded in the table. Here, the first stage evaluation of EBM is slightly changed by updating the equations as Eqs. (1) and (4) from the previous research (Kokusho & Mimori 2015); namely, the number of layers to liquefy has decreased from 12 to 11. SBM employing the stress reduction coefficient r_n =0.80 for the M=9.0 earthquake (Tokimatsu & Yoshimi1983) and the first stage EBM both predict that not only the hydraulic fill (F) but also B2 and As1 are to liquefy severely.

Following the results so far obtained in the first stage, induced strain is evaluated hereafter in the STEP-7 and 8 already mentioned. As the number of liquefiable layers determined in the STEP-7 is m=11, the upward energy allocated to individual layers are 1/11 of individual E_{UF} -values, from that the maximum induced shear strain γ_{DAmax} can be determined in Eq. (7) as listed in one of the right columns of Table 1 with bold letters. The induced strains assumed identical (γ_{DAmax} =7.5%) in all liquefied layers in the first evaluation stage are recalculated quite differently, from maximum 56.6% to minimum 4.4%. Consequently, the number

of layers beyond initial liquefaction became 6 (less than 11 of the first stage) because the equally-allocated upward energy tends to induce higher strains than 7.5% in weaker layers versus lower strains than that in stronger layers.

Next, volumetric strains ε_V are calculated by Eq. (9) as listed in Table 1 following STEP-9 by using $(\varepsilon_V)\gamma_{DAmax=20\%}=3.61\sim4.91\%$ determined by Eq. (8) according to N_1 and F_c (G_c can be assumed 0, here) in those layers which were judged to liquefy in the first evaluation stage. In one particular layer with $\gamma_{DAmax}=56.6\%$ exceeding the upper strain limit $\gamma_{DAmax}=20\%$., ε_V is calculated not by Eq. (9) but by Eq. (10). Then, the ground surface subsidence can be obtained in Eq. (11) as the sum of settlements of individual layers using H_i =1.0 m for all layers. Here, not only the strain $\gamma_{DAmax} > 7.5\%$ beyond initial liquefaction but also before that are involved in calculating the subsidence as long as they were judged liquefiable in the first evaluation stage.

The calculated subsidence 24.8 cm at the bottom of Table 1 seems to be smaller than the actual soil settlement, that was around 40 cm observed by the present author during his reconnaissance at a pile-supported school building as attached in Figure 4(a). However, the difference between the two values may possibly be much narrower because ejecta in large volume (more or less 10 cm thick) did actually occur to increase the ground subsidence in addition to the settlement calculated as the volume contraction solely by undrained cyclic loading.

6 SUMMARY

- To make the most of the energy-based method (EBM) already developed for simplified liquefaction evaluation, a stepwise methodology has been proposed to evaluate not only the occurrence of liquefaction but also induced strain and associated soil settlement by using experiment-based relationships.
- 2) This has become possible by first implementing the evaluation already proposed (where layers corresponding to initial liquefaction for γ_{DAmax} =7.5% are selected), and then by conducting the second stage evaluation wherein a simple assumption is introduced that the upward wave energy is equally allocated to all the liquefied layers already selected.
- 3) By applying this to a case history site, it has been found that the two-stage evaluation tends to lead to larger strains in smaller number of weaker layers than in the first stage, and lessen the number of layers going beyond initial liquefaction. It may well be expected that this second stage evaluation assuming the equal energy allocation to liquefied layers will be able to approach not exactly but nearer to actual liquefaction behaviour than in the first evaluation stage where equal strain of γ_{DAmax} =7.5% was assumed in all liquefied layers.
- 4) Furthermore, soil subsidence has been calculated from the induced shear strain in a case history site using a robust correlation of volumetric strain versus shear strain based on numerous triaxial liquefaction tests of various intact soils. The ground surface settlement thus calculated seems to be coincidental with the post-earthquake observation if the contribution of ejecta is considered.
- 5) Thus, the newly developed two-stage EBM seems to be able to predict not only a possibility of liquefaction but also an intensity of liquefaction in terms of maximum induced strains in liquefied layers and furthermore associated soil settlement with practical reproducibility, without resorting to complicated nonlinear effective stress dynamic response analyses, though more validations using much more case history data are certainly needed to confirm its applicability.

7 ACKNOWLEDGMENTS

Dr. Tomohiro Ishizawa, Senior Investigator of National Research Institute for Earth Science and Disaster Resilience, Tsuk uba, Japan, who kindly has long supported a series of research in developing design methods using the earthquake energy concept is gratefully acknowledged.

8 REFERENCES

- Davis R. O. and Berrill J. B. 1982. Energy Dissipation and Seismic Liquefaction of Sands, *Earthquake Engineering & Structural Dynamics* 10, 59-68.
- Ishihara K. and Yoshimine M. 1992. Evaluation of settlements in sand deposits following liquefaction during earthquakes, *Soils and Foundations* 32, 173-188.
- Japan Road Association 2017. Specifications for highway bridges-Part V Seismic Design-, Japan Road Association, (in Japanese).
- JGS committee report 2019. Research Committee on Liquefaction Potential Evaluation based on Energy, Japanese Geotechnical Society (in Japanese).
- Kazama M., Suzuki T. and Yanagisawa E. 1999. Evaluation of dissipated energy accumulated in surface ground and its application to liquefaction prediction, *Journal of Japan Society for Civil Engineers* (in Japanese), JSCE 631/III-48, 161-177.
- Kokusho T. 2013. Liquefaction potential evaluation–energybased method versus stress-based method-, Canadian Geotechnical Journal 50, 1-12.
- Kokusho T. and Mimori, Y. 2015. Liquefaction potential evaluations by energy-based method and stress-based method for various ground motions, Soil Dynamics & Earthquake Engineering 75, Elsevier, 130–146.
- Kokusho T. 2017. Liquefaction potential evaluations by energybased method and stress-based method for various ground motions: Supplement, Soil Dynamics & Earthquake Engineering 95, Elsevier, 40–47.
- Kokusho T. 2017. Innovative Earthquake Soil Dynamics, *CRC Press*, Chapter 5: Liquefaction.
- Kokusho T. and Kaneko Y. 2018. Energy evaluation for liquefaction-induced strain of loose sands by harmonic and irregular loading tests, Soil Dynamics & Earthquake Engineering 114, 362–377.
- Sasaki T., Ishihara M., Tanimoto S., Hayashi H., Egawa T., Washimi K., and Kawaguchi G. 2016. *PWRI Research Note* 4352, Public Works Research Institute (in Japanese).
- Tanimoto S. and Kokusho T. 2020. Empirical correlation between liquefaction energy capacity and cyclic resistance ratio for in-situ intact samples, *JGS Journal (Special Issue)* 15 (1), The Japanese Geotechnical Society (in Japanese), 25-38.
- Tokimatsu K. and Yoshimi Y. 1983. Empirical correlation of soil liquefaction based on SPT N-value and fines content, *Soils and Foundations* 23 (4), 56-74.